JOURNAL OF COMPUTATIONAL PHYSICS 79, 231–243 (1988)

Note

Comparison of Finite Differences and Finite Elements on a Parabolic Problem*

In a previous article [1], Shestakov *et al.* compared numerical solutions of the diffusion equation using two distinct methods, a nodal one using finite elements, FE, and a zonal one based on finite differences, FD. The FD method has been described in an earlier paper by Kershaw [2]. In Ref. [1], emphasis was placed on obtaining an accurate solution on a "random mesh," a prototype of what might be created by Lagrangian hydrodynamic distortions. In this note a similar comparison is made, but attention is turned to a smooth, nearly orthogonal mesh. The next paragraph presents a function that generates the grid. Two meshes, one a refinement of the other, are considered in this paper. They are used to solve two simple test problems. The first models linear energy diffusion through optically thick material. In the second problem, the material is optically thin and a flux limiter is invoked. The analytic solutions are one dimensional, but the numerical results show the effects of the mesh.

To construct the grid consider the mapping:

$$R = s + \alpha \sin(\pi s)\cos(\pi t) \tag{1a}$$

$$Z = t - \alpha \sin(\pi t)\cos(\pi s). \tag{1b}$$

If $\alpha \leqslant 1/\pi$, then for $0 \leqslant s, t \leqslant 1$, Eq. (1) implies $0 \leqslant R, Z \leqslant 1$. Given two integers *KMAX* and *LMAX*, a mesh may be generated by first defining two arrays, $[s_L]_{L=1}^{LMAX}$ and $[t_K]_{K=1}^{KMAX}$, where

$$s_L = \frac{L-1}{LMAX-1} \quad \text{and} \quad t_K = \frac{K-1}{KMAX-1}. \tag{2}$$

* This work was performed under the auspices of the U. S. Department of Energy by the Lawrence Livermore National Laboratory under Contract W-7405-ENG-48. This document was prepared as an account of work sponsored by an agency of the United States Government. Neither the United States Government nor the University of California nor any of their employees, makes any warranty, express or implied, or assumes any legal liability or responsibility for the accuracy, completeness, or usefulness of any information, apparatus, product, or process disclosed, or represents that its use would not infringe privately owned rights. Reference herein to a specific commercial products, process, or service by trade name, trademark, manufacturer, or otherwise, does not necessarily constitute or imply its endorsement, recommendation, or favoring by the United States Government or the University of California. The views and opinions of authors expressed herein do not necessarily state or reflect those of the United States Government or the University of California, and shall not be used for advertising or product endorsement purposes.

0021-9991/88 $3.00

These arrays in turn generate the mesh points $(R_{K,L}, Z_{K,L})$. For the test problems, the mesh of Eqs. (1) and (2) is translated by one in the R direction. The domain: $0 \leqslant Z \leqslant 1$, $1 \leqslant R \leqslant 2$ is first filled with a square logical grid, $(KMAX = LMAX)$. Next, two additional row of zones are placed below $R = 1$ and above $R = 2$. The final grid has $LMAX = KMAX + 2$; an example of a 33×35 mesh is displayed in Fig. 1 where $\alpha = 1/3.2$. The lines $K = 1, KMAX$ coincide with $Z = 0, 1$ respectively while the lines $L = 1, LMAX$ coincide with $R = 1 - \Delta_{KMAX}, 2 + \Delta_{KMAX}$ respectively where $\Delta_{KMAX} \equiv 1/(KMAX - 1)$. We compare results along $L = LMAX$ (i.e., along $R_1 \equiv 2 + \Delta$) and especially at the $(2, LMAX)$ and $(KMAX, LMAX)$ zones (the zones are labeled by the largest value of the K and L indices of any of its vertices). Only grids corresponding to $KMAX = 33$ or 65 and $\alpha = 1/3.2$ are considered in this paper.

The mapping of Eq. (1) is invertible, for its Jacobian equals

$$J = \frac{\partial(R, Z)}{\partial(s, t)} = 1 - (\alpha\pi)^2 [\sin^2(\pi s) + \sin^2(\pi t) - 1] \tag{3}$$

and is nonzero if $\alpha < 1/\pi$. It is easy to analyse how far the mesh strays from

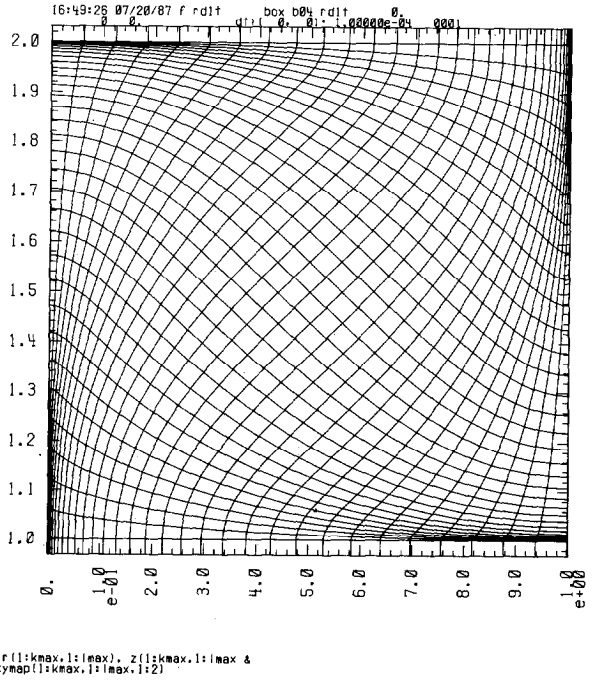

FIG. 1. Computational 33×35 mesh. Z is the abscissa, R the ordinate; K increases with Z, L increases with R.

orthogonality. The grid generated by Eqs. (1) and (2) is a contour plot of constant s and t values and

$$\begin{bmatrix} dR \\ dZ \end{bmatrix} = \mathbf{J} \begin{bmatrix} ds \\ dt \end{bmatrix}, \tag{4}$$

where the elements of the Jacobian matrix, $\mathbf{J}$, consist of the corresponding partial derivatives of Eq. (1), e.g., $R_s \equiv \partial R/\partial s$. Multiplying Eq. (4) by $\mathbf{J}^{-1}$ expresses the changes of s and t in terms of changes of R and Z. Then it is trivial to compute the normalized gradient vectors,

$$\hat{\mathbf{n}}_s = \frac{\nabla s}{|\nabla s|} = \frac{(Z_t, -R_t)}{\sqrt{Z_t^2 + R_t^2}}, \qquad \hat{\mathbf{n}}_t = \frac{\nabla t}{|\nabla t|} = \frac{(-Z_s, R_s)}{\sqrt{Z_s^2 + R_s^2}}. \tag{5}$$

The gradient vectors are in the R and Z directions respectively, e.g., $\nabla s = J^{-1}(Z_t \hat{\mathbf{R}} - R_t \hat{\mathbf{Z}})$. The normalized gradients of Eq. (5) are normal to the $s, t = \text{const}$ curves of Fig. 1; their product calibrates the degree of orthogonality of the mesh. Substituting the mapping of Eq. (1) we write this product in compact form:

$$f(s, t) \equiv \hat{\mathbf{n}}_s \cdot \hat{\mathbf{n}}_t = \left\{ 1 + 4 \left[\frac{1 - (\alpha\pi)^2 (\cos 2\pi s + \cos 2\pi t)/2}{(\alpha\pi)^2 \sin 2\pi s \sin 2\pi t} \right]^2 \right\}^{-1/2}. \tag{6}$$

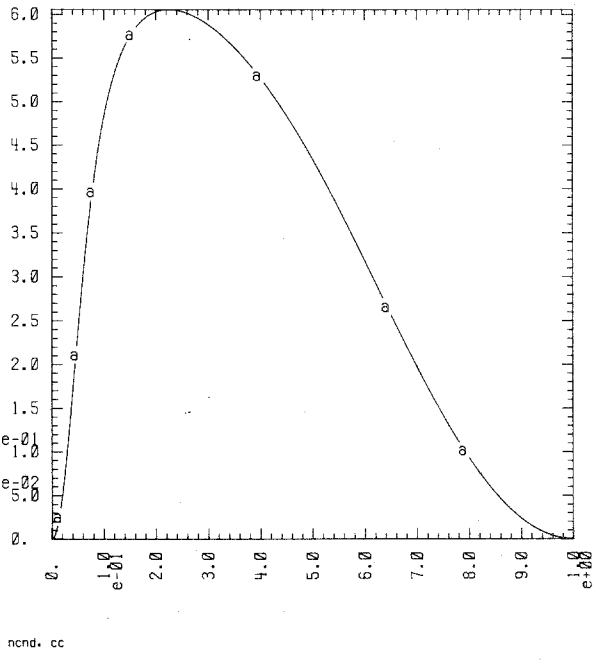

FIG. 2. Measure of orthogonality of the mesh, $f(s, s)$, as a function of the abscissa, $2s$.

Since f is symmetric in s and t, its extrema occur when $s=t$ and so we examine the function $f(s, s)$. Using $2s$ as the independent variable, $f(s, s)$ is displayed in Fig. 2. It vanishes at $s=0, \frac{1}{2}$ and peaks at $s\approx 0.115$, where $f_{\max}\approx 0.605$. On a 33×33 grid this translates into a minimum angle of approximately 53° at $K=L\approx 4$. Mapping to the R, Z space of Fig. 1, the grid lines deviate the most from orthogonality at $(R, Z)\approx(1.22, 0.012)$ and the other 3 points symmetric to it.

The above grid is used to solve the energy conduction equation,

$$\partial_t u=\frac{1}{R}\partial_R(RD\,\partial_R u) \tag{7}$$

on the domain: $1-\Delta\leqslant R\leqslant R_1\equiv 2+\Delta$ and $0\leqslant Z\leqslant 1$. In Eq. (7) and in what follows t denotes time and u is an energy density. The diffusion coefficient, D, is a function of the mean free path, l. As an initial condition, we set $u=1.372\times 10^{-26}$. A Milne or mixed boundary condition,

$$u+\frac{2l}{3}\partial_R u=0, \tag{8}$$

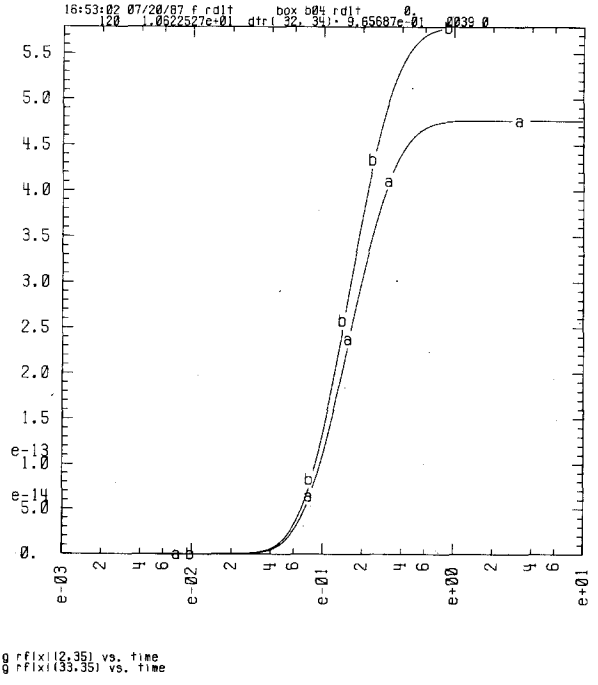

FIG. 3. Linear energy conduction problem; FD scheme; 33×35 mesh. Outgoing flux near $(R, Z)=(2, 0)$ (curve "a") and outgoing flux near $(R, Z)=(2, 1)$ (curve "b") as functions of time.

is imposed along R_1. Symmetry conditions hold along the Z boundaries. At time $t=0$ and thereafter we fix $u=u_0=7.042\times10^{-13}$ along $R=R_0\equiv1$. A caveat: for the nodal FE scheme, u is fixed along $R=R_0$ and $R_0-\Delta$. For the zonal FD scheme, u is fixed along the lowest set of zones: $1-\Delta\leqslant R\leqslant1$ which effectively fixes u at some intermediate zone centers, $\tilde{R}_0$, [2] obtained by integrating over the above R range:

$$\tilde{R}_0=\frac{\int R^2\,dR}{\int R\,dR}=\frac{1-\Delta+\Delta^2/3}{1-\Delta/2}. \tag{9}$$

Hence, $\tilde{R}_0=0.9845$, 0.9922 if $KMAX=33$, 65, respectively.

We model the radial duffusion of a constant energy source. Energy is measured in units of $J=10^{16}$ ergs. Time is in units of $\tau=10^{-8}$ s. Distances are in centimeters. Hence, u, the energy density, is in units of J/cm^3, the speed of light, $c\approx300\,\text{cm}/\tau$, and the constant density ρ is in units of grams/cm^3. Some results are given in terms of the energy per gram, E_r; clearly, $u=\rho E_r$. The mean free path is given by

$$l=1/\rho\kappa, \tag{10}$$

and the opacity, κ (cm^2/g) is fixed, $\kappa=1$.

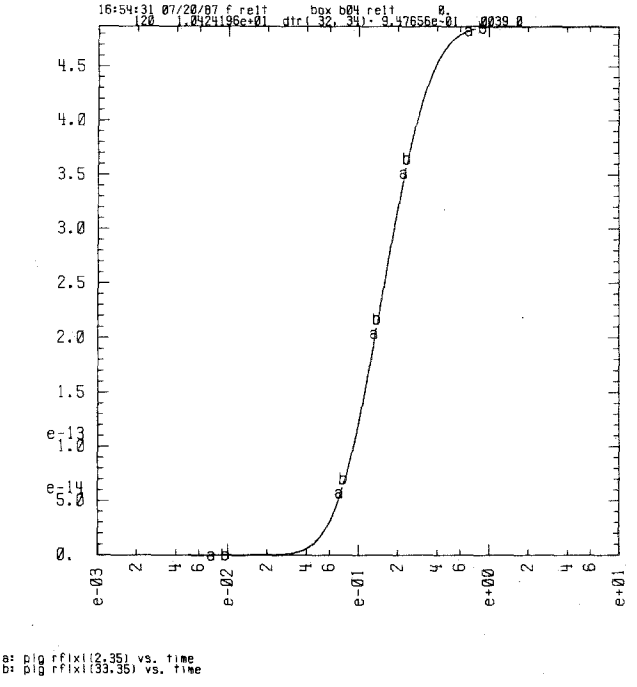

FIG. 4. Linear energy conduction problem; FE scheme; 33×35 mesh. Outgoing flux near $(R, Z)=(2, 0)$ (curve "a") and outgoing flux near $(R, Z)=(2, 1)$ (curve "b") as functions of time.

In the first problem, linear energy conduction is modeled,

$$D=\frac{cl}{3}, \tag{11}$$

and $l=10^{-2}$ ($\rho=10^2$). From Eq. (7), the characteristic diffusion equilibration time is given by

$$\frac{u}{t_D}\approx\frac{Du}{d^2}, \qquad \text{hence} \quad t_D\approx\frac{d^2}{D}, \tag{12}$$

where $d=1$ is the characteristic gradient length of the problem. Substituting, we find $t_D\approx 1$.

This simple argument is accurate to within an order of magnitude. In Figs. 3 and 4 we plot the time history of the outgoing flux in units of J/cm^2/τ for the (2, LMAX) and (KMAX, LMAX) zones for the FD and FE methods. Note that by $t=t_D$, the flux has stabilized to its equilibrium value. Figure 3 (FD scheme) shows that near $(R, Z)=(2, 1)$, the flux is 17% greater than at $(R, Z)=(2, 0)$. The FE results of Fig. 4 show no such asymmetry. The bias of FD is entirely due to mesh effects. It is systematic over the problem duration time. It anomalously and

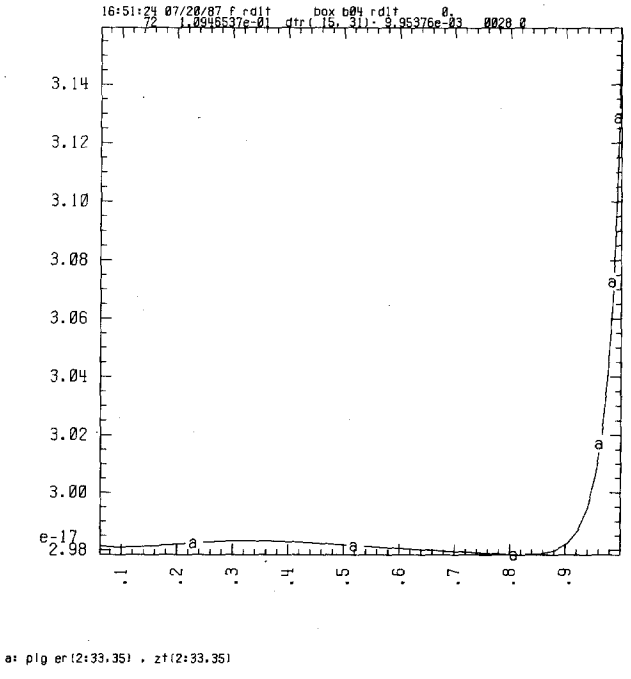

FIG. 5. Linear energy conduction problem; FD scheme; 33×35 mesh. Zonal energy per gram, E_r, as a function of Z at the outgoing boundary, $R=R_1$.

consistently raises the energy in the $(R, Z) = (2, 1)$ corner. Figures 5 and 6 plot E_r along R_1 at $t \approx 0.1$ which according to Figs. 3 and 4 corresponds to the time of arrival of the energy front. The FD results of Fig. 5 show that the energy at $Z = 1$ is 6% larger than at $Z = 0$. The FE results of Fig. 6 show only

$$\frac{E_{r,\max}}{E_{r,\min}} = 1.004 \tag{13}$$

or a 0.4% variation. Furthermore, the oscillations do not depend on the continuous mesh distortions.

We conclude this problem by comparing the accuracy of the results. The boundary conditions imply that the equilibrium solution is

$$u_e = u_0 \frac{1 + (3R_1/2l)\log(R_1/R)}{1 + (3R_1/2l)\log(R_1/R_0)}. \tag{14}$$

The outgoing flux along $R = R_1$ is

$$-D\nabla u = \frac{cl}{3}\partial_R u = cu_0/2 \Big/ \left(1 + \frac{3R_1}{2l}\log\left(\frac{R_1}{R_0}\right)\right). \tag{15}$$

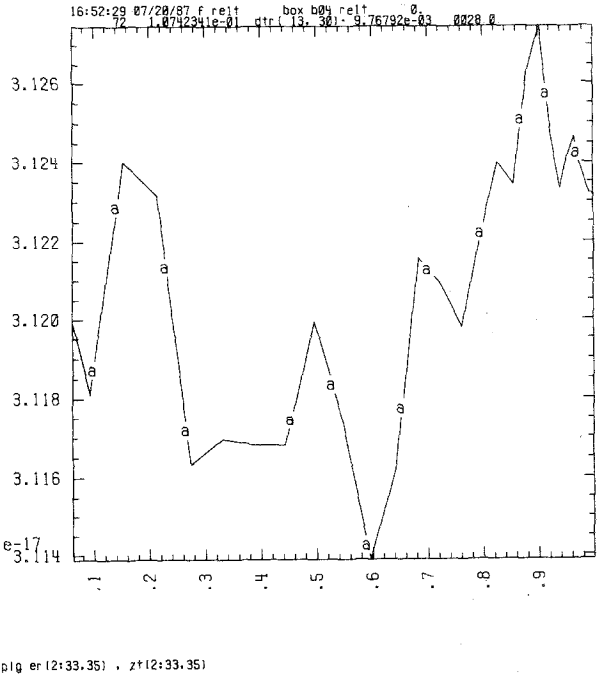

FIG. 6. Linear energy conduction problem; FE scheme; 33×35 mesh. Zonal energy per gram, E_r, as a function of Z at the outgoing boundary, $R = R_1$.

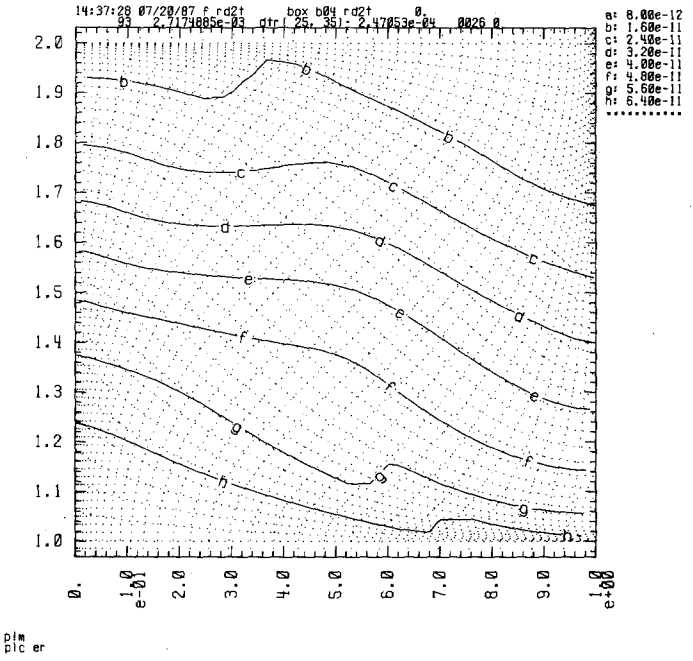

FIG. 7. Flux limited conduction problem; FD scheme; 33×35 mesh. Contours of zonal energy per gram, E_r. Dotted lines denote the grid. Time of plot ($\approx 2.717 \cdot 10^{-3}$) is approximately $\frac{3}{4}$ of the light transit time t_c.

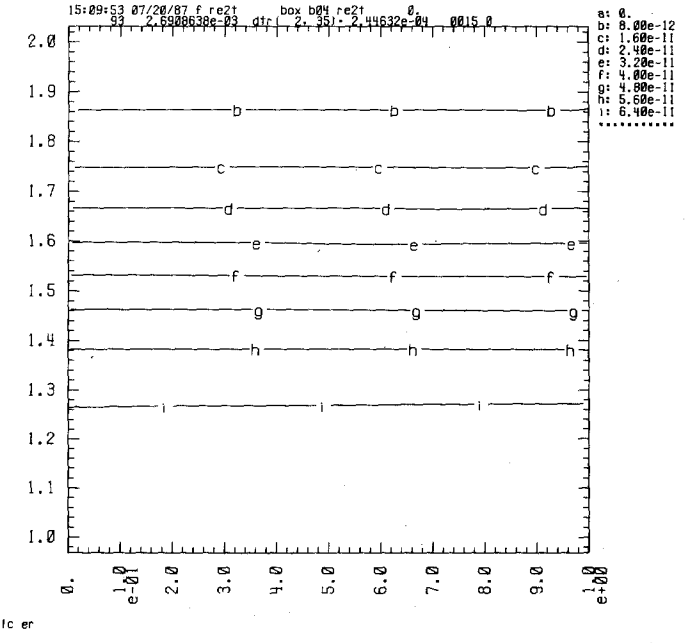

FIG. 8. Flux limited conduction problem; FE scheme; 33×35 mesh. Contours of zonal energy per gram, E_r. Time of plot ($\approx 2.691 \cdot 10^{-3}$) is approximately $\frac{3}{4}$ of the light transit time t_c.

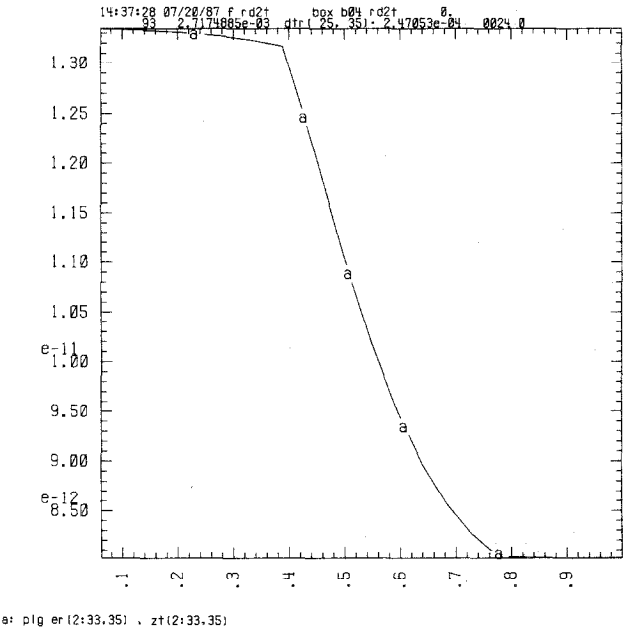

FIG. 9. Flux limited conduction problem; FD scheme; 33×35 mesh. Zonal energy per gram, E_r, as a function of Z at the outgoing boundary, $R = R_1$. Time of plot ($\approx 2.717 \cdot 10^{-3}$) is approximately $\frac{3}{4}$ of the light transit time t_c.

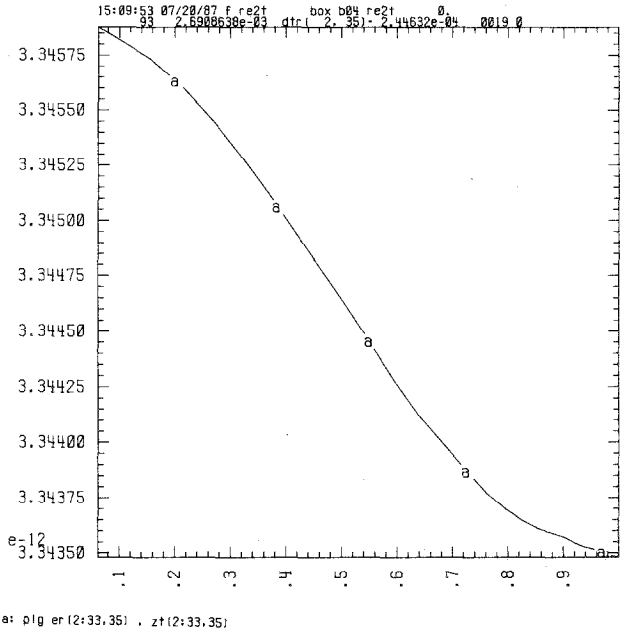

FIG. 10. Flux limited conduction problem; FE scheme; 33×35 mesh. Zonal energy per gram, E_r, as a function of Z at the outgoing boundary, $R = R_1$. Time of plot ($\approx 2.691 \cdot 10^{-3}$) is approximately $\frac{3}{4}$ of the light transit time t_c.

Substituting, we obtain $D\nabla u = 4.8662 \times 10^{-13}$, 4.9577×10^{-13} if $KMAX = 33$, 65, respectively (for $R_0 = 1$). These values should be suitably modified for FD if using $\tilde{R}_0$. If $KMAX = 33$, the equilibrium FE fluxes vary between 4.8708×10^{-13} and 4.8631×10^{-13} or 0.15%; the FD fluxes vary between 5.792×10^{-13} and 4.760×10^{-13} or 21%. Even for KMAX = 65, the FD fluxes have large asymmetries, they vary between 5.217×10^{-13} and 4.904×10^{-13} or 6.4%; the corresponding FE fluxes vary between 4.95965×10^{-13} and 4.95685×10^{-13} or 0.06%. The superiority of FE is self-evident.

The second test problem exhibits an even greater difference between the two methods. We change ρ to $\rho = 10^{-2}$ and thereby increase l to $l = 10^2$. The domain is now optically thin as $l \gg d$. For this case, radiation diffusion theory is strictly invalid and one should properly use the full transport equations [3]. However, in many applications, the reduced dimensionality of the diffusion equations has an irresistible appeal and so they are still used in a modified form with a flux-limited diffusion coefficient. The flux limiter has an effect whenever the light transit time,

$$t_c \equiv \frac{d}{c} > t_D. \tag{16}$$

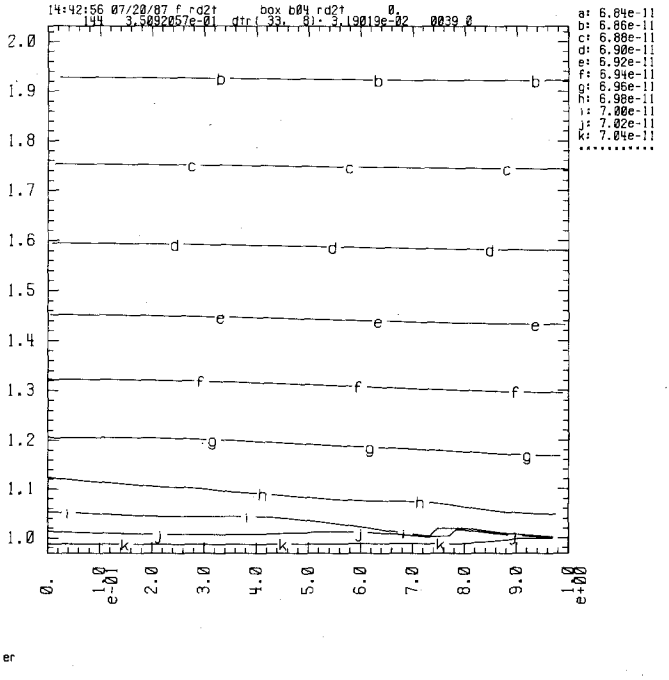

FIG. 11. Flux limited conduction problem; FD scheme; 33 × 35 mesh. Equilibrium contours of zonal energy per gram, E_r.

For this problem, $d \approx 1$, hence,

$$t_c \approx 3.33 \cdot 10^{-3} > t_D \approx 10^{-4}. \tag{17}$$

The flux limiter attempts to limit the velocity of propagation of the energy front to c. The flux limited diffusion coefficient used is

$$D = c/\max(3/l, |\nabla u|/u) \tag{18}$$

and is invoked explicitly. Its effectiveness is seen by examining the energy at $t = 2.7 \times 10^{-3}$. Since this is less than t_c, the energy along $R = R_1$ should be unaffected by the source along R_0. The results emphasize the shortcomings of diffusion theory and comparison of the numerical results illustrate the respective influences of the mesh. Contours of E_r are displayed in Figs. 7 and 8 for the FD and FE schemes respectively ($KMAX = 33$). Figure 7 also displays the mesh with dotted lines. The FD deviation from the expected Z symmetry is clearly due to the mesh. Figures 9 and 10 display E_r along R_1. In Fig. 9, the FD scheme shows a 58% variation; the FE results of Fig. 10 show only a 0.07% variation. Even the equilibrium contours of the FD scheme are poor; they are displayed in Fig. 11. The analytic equilibrium flux along $R_1 = 2 + \Delta_{33}$ is 1.0333×10^{-10}. The FE results along R_1 equal

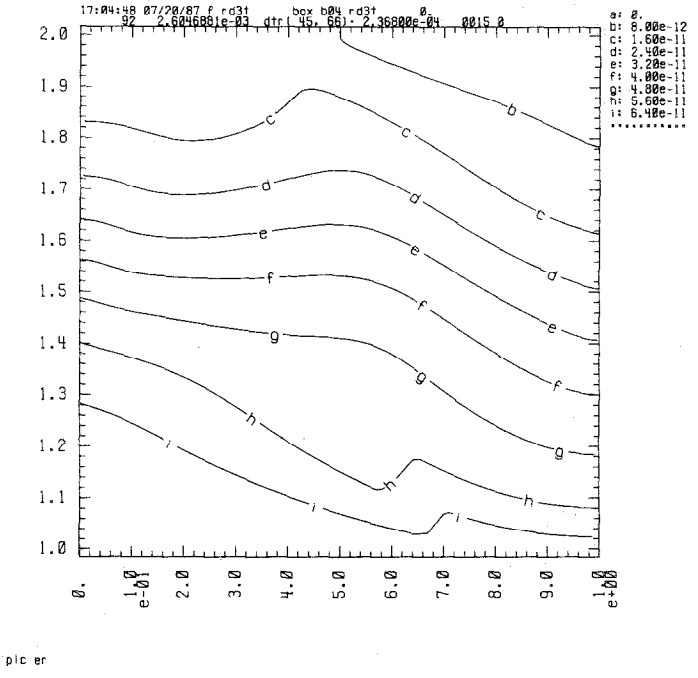

FIG. 12. Flux limited conduction problem; FD scheme; 65×67 mesh. Contours of zonal energy per gram, E_r. Time of plot ($\approx 2.605 \cdot 10^{-3}$) is approximately $\frac{3}{4}$ of the light transit time t_c.

1.0336×10^{-10} and are the same for at least 7 figures. The corresponding FD equilibrium fluxes have an 11% variation. They rise steeply at the $(R, Z) = (2, 1)$ corner.

The FD results do not improve on the finer ($KMAX = 65$) mesh. Contours of E_r for FD at $t \approx 2.6 \times 10^{-3}$ are given in Fig. 12. Figure 13 plots E_r along R_1, a 117% variation appears. For comparison, the FE results on the finer mesh at $t \approx 2.7 \cdot 10^{-3}$ have a 0.1% variation. The equilibrium FD fluxes along R_1 have a 3.7% variation while the FE fluxes are nearly constant in Z.

We conclude that FE is superior for transport dominated problems. This was previously demonstrated on random meshes and the results of this article show that even for smoothly varying grids, mesh effects may be dominant for FD while being nearly negligible for FE. Mesh effects are unavoidable for they will arise from the grid generated at the start of the calculation. Such nonorthogonalities appear when the mesh is aligned with a portion of the boundary or when the mesh is refined to elicit greater accuracy from a portion of the domain. The results of this article demonstrate that such grids may have an unphysical influence on the calculation when using finite differences. Yet such errors may be especially difficult to isolate on more general problems. These inaccuracies are not characterized by classical

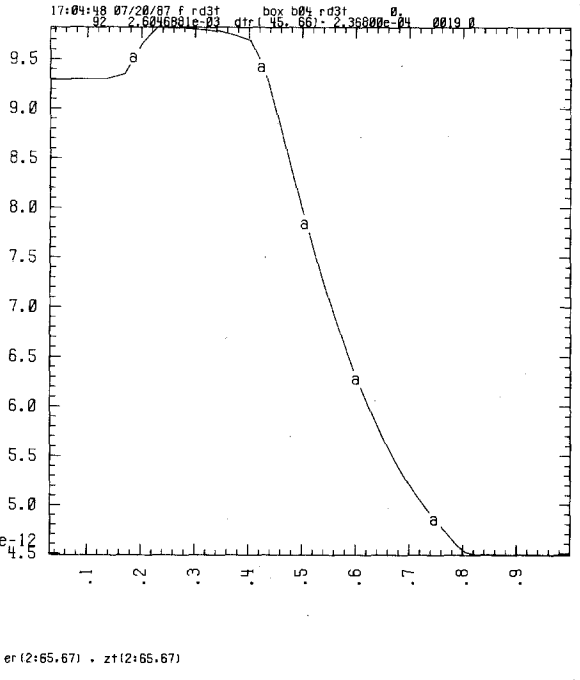

FIG. 13. Flux limited conduction problem; FD scheme; 65×67 mesh. Zonal energy per gram, E_r, as a function of Z at the outgoing boundary, $R = R_1$. Time of plot ($\approx 2.605 \cdot 10^{-3}$) is approximately $\frac{3}{4}$ of the light transit time t_c.

numerical instabilities that alert the user. The FD answers look smooth, but are nevertheless incorrect. Lastly, we note that for nonorthogonal grids, both FD and FE require similar amounts of computational effort as they are both nine-point schemes.

REFERENCES

1. A. I. SHESTAKOV, J. A. HARTE, AND D. S. KERSHAW, Lawrence Livermore National Laboratory Report, UCRL 95066, *J. Comput. Phys.*, in press.
2. D. S. KERSHAW, *J. Comput. Phys.* **39** No. 2, 375 (1981).
3. G. C. POMRANING, *Radiation Hydrodynamics* (Pergamon, Oxford, 1973).

RECEIVED: August 20, 1987; REVISED: December 22, 1987

A. I. SHESTAKOV

Computational Physics Division
Lawrence Livermore National Laboratory
P. D. Box 5508, Livermore, California 94550